Developing Infrared Thermography as an Instructional Tool for Monitoring Energy Efficiency Issues in Micro-Manufacturing

Dr. Richard Chiou, Drexel University
Dr. Michael G Mauk P.E., Drexel University
Prof. Tzu-Liang Bill Tseng, University of Texas, El Paso

Tzu-Liang (Bill) Tseng is an associate professor of Industrial, Manufacturing and Systems Engineering at University of Texas at El Paso (UTEP). He received his M.S. degree in Decision Sciences at University of Wisconsin-Madison and his Ph.D. degree in Industrial Engineering at University of Iowa. His research focuses on the computational intelligence, data mining, bio- informatics and advanced manufacturing. Dr. Tseng published in many refereed journals such as IEEE Transactions, IIE Transaction, Journal of Manufacturing Systems and others. He has been serving as a principle investigator of many research projects, funded by NSF, NASA, DoEd, and KSEF. He is currently serving as an editor of Journal of Computer Standards & Interfaces.

Mr. M. Eric Carr, Drexel University

Mr. Eric Carr is a full-time Laboratory Manager and part-time adjunct instructor with Drexel University's Engineering Technology program. Eric assists faculty members with the development and implementation of various Engineering Technology courses. A graduate of Old Dominion University's Computer Engineering Technology program and Drexel's College of Engineering, Eric enjoys finding innovative ways to use microcontrollers and other technologies to enhance Drexel's Engineering Technology course offerings. Eric is currently pursuing a Ph.D in Computer Engineering at Drexel, and is an author of several technical papers in the field of Engineering Technology Education.

Aurel Mathews

Developing Infrared Thermography as an Instructional Tool for Monitoring Energy Efficiency Issues in Micro-Manufacturing

Abstract

Instruction in the basic engineering disciplines of energy efficiency and process control can be enhanced and expanded by incorporating various imaging capabilties into experiments and projects used to teach the concepts and practice of these subjects. Image capture, image processing, and image analysis offer means for visualization of phenomena and processes, and enable convenient and more expansive measurement capabilities to characterize and analyze fluid motion, phase transitions, and various thermal phenomena. Infrared imaging (thermography) offers new capabilities for measurements and analyses, as well as unprecedented means for visualization as an aid in learning science and technology in micro-manufacturing. Moreover, infrared thermography is becoming a commonplace— if not essential —tool in process control and analysis, quality assurance, non-destructive testing, materials characterization, and reliability; and in our view should therefore take a more prominent place in engineering education. For green manufacturing and sustainability, infrared imaging can be used to reduce waste and energy consumption, assess the performance of new energy conversion technologies, characterize heat and mass transfer in microscale devices, and support or enable more quantitative and objective metrics in product life cycle management. Educational institutions seeking to incorporate thermography in their curricula can benefit from a new generation of infrared imaging cameras that are comparatively inexpensive, easier to use, and more functional, as well as free-ware and widely available commercial image processing software (ImageJ, MATLAB). The paper presents an effort on developing educational laboratory projects with an infrared imaging analysis component for compatibility with course delivery by remote access via the web, or in traditional lecture and hands-on laboratory format.

Background

Instruction in the basic engineering disciplines of heat and mass transfer, fluid mechanics, and process control can be enhanced and expanded by incorporating various imaging capabilties into experiments and projects used to teach the concepts and practice of these subjects. Image capture, image processing, and image analysis offer means for visualization of phenomena and processes, and enable convenient and more expansive measurement capabilities to characterize and analyze fluid motion, phase transitions, and various thermal phenomena. Further, these experiments can implemented in microsystems that can be readily fabricated using rapid prototyping tools, and instrumented with microcontrollers or laboratory automation systems such as LabVIEW™. Thus, hands-on projects to supplement foundation engineering courses can productively combine elements of microsystems (lab on a chip microfluidic devices), computer-aided design and rapid prototyping, image capture and analysis, sensors and microcontrollers. These projects can be run on a lab bench or desktop, are relatively inexpensive to implement and maintain, are comparatively safe to operate, and generate little in the way of waste materials or other environmental hazards. Such approaches to engineering educational laboratories follow trends in chemistry education employing microscale laboratories in place of the traditional wet chemistry (e.g., flasks and beakers) experiments. Moreover, the student is fully engaged in all aspects of the experiments (design, fabrication, instrumentation, operation, data acquisition and analysis)[1-4].

Thermal (infrared) imaging and machine vision are increasingly important and versatile technologies for research, production, and energy efficiency in general, and for sustainable 'green' manufacturing and renewable energy in particular. Virtually any process where temperature is an important consideration can be explored and monitored with a thermal camera. Machine vision (image capture, processing and analysis---both infrared and visible) can be used for process control and automation, quality assurance, diagnostics, materials assessment, and identication of energy losses. Thermal imaging is an especially an effective vehicle for teaching science and engineering. Thermography methods are now used in many engineering disciplines and technologies. For instance, effects related to heating and heat transfer, phase transitions, convection, friction, and other dissipitive processes can be visualized with thermal imaging. Images provide much useful data for characterization and assessment; process identification, optimization, and control; quality metrics, elucidating failure mechanisms and other reliability issues, and reducing waste and energy consumption in sustainable and green manufacturing[5-8].

We surveyed the types of infrared cameras available, based on technically adequacy, operational simplicity, cost, and durability, as relevant to their use in engineering education. Cameras that operate in the 8 to 12 micron spectral region, and have a resolution of about ±1.0 °C range in cost from about $1000 to 20,000. The chief cost discriminator is image pixel size. A camera costing between $2000 and $10,000, such as a FLIR Model 360 camera with 320 x 240 pixel image size, should suffice for most educational laboratory projects. We will develop remote access use of the camera so that other schools without cameras can share equipment and perform the image capture experiments over the internet[9-13].

Microfluidic Heat Exchanger

A representitive experiment uses an infrared camera to capture the two-dimensional temperature profile of a microfluidic heat exchanger. This experiment will introduce students to the techniques of infrared imaging. Its subject of analysis is a microsystem instrumented with sensors and hosting microfluidic 'circuits' carrying heated liquids. The fluid flow can also be imaged with a visible imaging camera to make videos of the flow, and quantify flow characteristics. This shows the complementary and supplemental information provided by imaging in two spectral regions. Such microsystems are of technical interest for *lab-on-a-chip* technologies which seek to provide miniature, sustainable implementations of fluidic processes that are traditionally implemented on laboratory benches, or pilot plants at much larger scale. These systems will reduce consumption of materials, generation of waste, and use of energy. Further, they are amenable rapid prototyping and so can speed product development times. These systems also simulate conventional fluid and thermal systems but on a microscale. They will allow educational institutions to substitute these desktop microscale systems for tradtional laboratory equipment that normally is a factor of 10 or more greater in floor space, capital and operating costs, and create certain safety and enviromental issues. Clearly such miniaturization is a dominant theme of sustainable green manufacturing and product development, and our imaging experiments will give students much experience in many aspects of microscale engineering. Further, their low impact in cost, space, and other resources will facilitate their dissemination to many educational institutions.

The microfluidic chips are designed with AutoCAD™ or SolidWorks™ (Figure 1a). The chips are fabricated as laminates. A middle layer is machined with through cuts to define the fluidic circuit in a thin (1 mm) sheet of plastic using a laser cutter or CNC machine (Figure 1b). The channels and

chambers of the middle layer are enclosed by attaching top and bottom plastic sheet layers using thermal bonding, solvent bonding, adhesives, or special double-sided tapes. Samples and reagents can be pipetted directly into the chip or extracted from the chip through inlet/outlet ports. Alternatively, fluidic interconnections are provided by small-diameter (Teflon) tubing inserted through sidewall ports of the chip. We also found disposable pipette tips (e.g., Denville Sharp™ precision barrier tips), shorted by cutting off the tip and with fibrous plug removed, made good transitions between tubing and chip ports (drilled holes). The tubing and sideport hole diameters are selected to make a snug, leak-tight fit. Using tubing interconnections, the liquids can be delivered to the fluidic circuit with a pipette or a syringe, actuated either manually or with a programmable syringe pump.

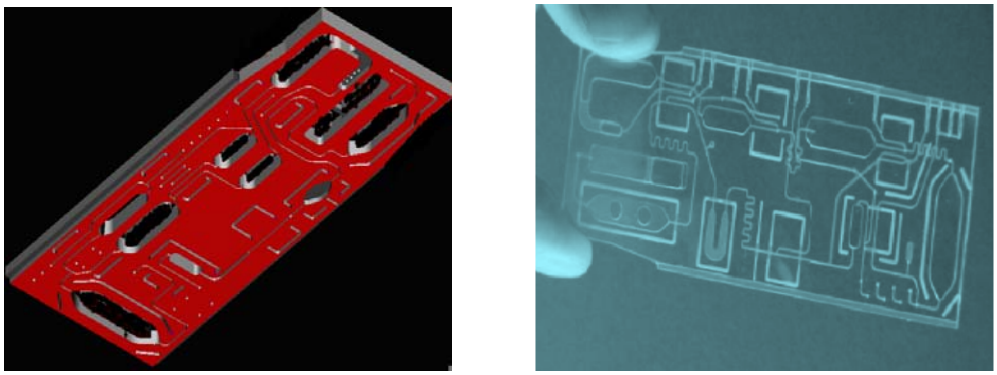

(a) (b)

Figure 1: (a) SolidWorks desgin of chip and (b) fabricated chip in acrylic

Chip Design and Manufacturing

The microfluidic chips are fabricated as three layer laminates comprised of a middle layer that featured the fluidic circuit and top and bottom layers that enclosed it. The middle layer is designed in AutoCAD and then sent to a prototyping machine. It can be prototyped using several different methods but in this case a CO_2 laser cutter is used to define the fluidic circuit using through cuts. Plastic acrylic is the material of choice for the middle layer. The top and bottom layers of the chip consist of clear plastic sheets that are attached to both sides of the middle layer. There are several methods that can be used to attach these to the middle layer such as thermal bonding, solvent bonding, or by using adhesives.

Figure 2: AutoCAD™ desgin of chip for CO_2 laser chip cutting

The dimensions of the chip and the design of the microchannels are created using AutoCAD. Once completed, the chip design is saved as an AutoCAD dwg file. The file is sent to the laser system by selecting 'plot' and specifying the printer as 'VLS3.50'. The AutoCAD file then appears in the laser print driver, Laser Interface +. Laser Interface + allows for manual control over location, laser power, speed, and other system settings. After all the system parameters are set, the desired material is placed inside the CO_2 laser system to be cut. To provide links for fluidic interconnections, the inlet and outlet holes are drilled into the chip's sides by using a micro milling machine. Microfluidic interconnections are an important part of the system because they seal the chip's ports and allow for appropriate interfacing between other devices. The microfluidic interconnections need to provide with a tight, leak-proof fit so that the micropipette tips work properly.

As shown in Figure 3, the experimental setup consists of the microfluidic chip wherein a fluid enters at an inlet temperature and exits at an outlet temperature. A syringe pump causes the fluid to flow through the chip by pulling fluid from the fluid reservoir that is located on a hot plate at a constant temperature 175°C (although the temperature of the fluid in the reservoir was only measured to be approximately 75°C). A thermoelectric Peltier cooling device pumps heat from the cold side to the hot side where the fan circulates the ambient air between the heat sink's fins to absorb the collected heat. A DC regulated power supply provided power to the cooling fan and current to the thermoelectric cooler.

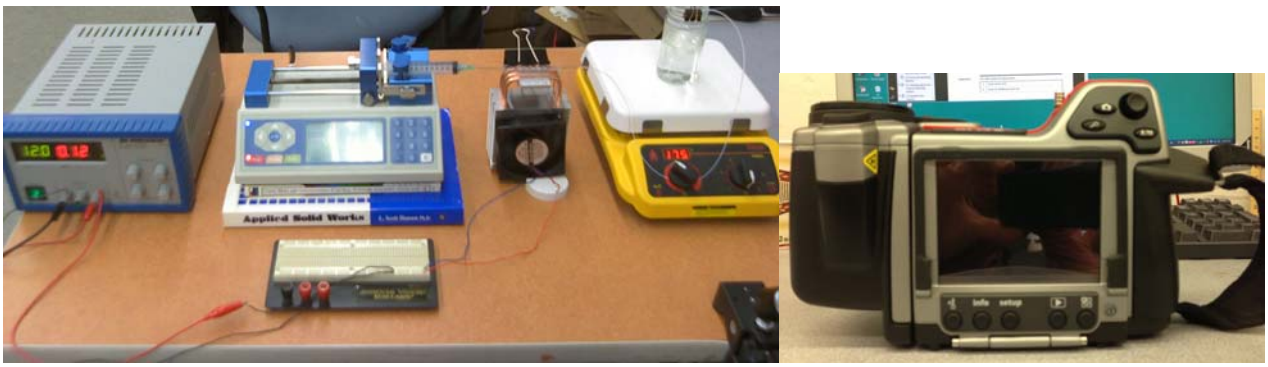

Figure 3: Experimental setup for infrared thermography of microfluidic chip

The experiments are carried out in two modes. In the first mode, the DC power supply is turned off to observe the heat transfer caused by syringe pump induced fluid flow through the chip. The DC power supply is turned on in the second mode to observe the heat transfer associated with the thermoelectric Peltier cooling device, heat sink, and cooling fan. For each mode, the syringe pump is set to three volumetric flow rates to be called low, medium, and high flow rate. The low, medium and high flow rates are 4000 µL/min, 5000 µL/min, and 6,000 µL/min, respectively. Although these are the values given by the syringe pump, they are not the actual flow rates due to disconformities between the syringe pump and the experimental system.

Peltier Effect

The Peltier effect is the concept behind thermoelectric cooling and it occurs when electrical current flows between two dissimilar conductors (Figure 4). The two types of semiconductors used are doped to create an excess (N-type) or a lack (P-type) of free electrons. The two types of semiconductors are

arranged in a couple and wired in series with a plated copper tab to keep heat moving in the same direction. As current passes through the thermoelectric cooler, heat is pumped from the cold side to the hot side. The amount of heat absorbed is directly proportional to the current and its duration.

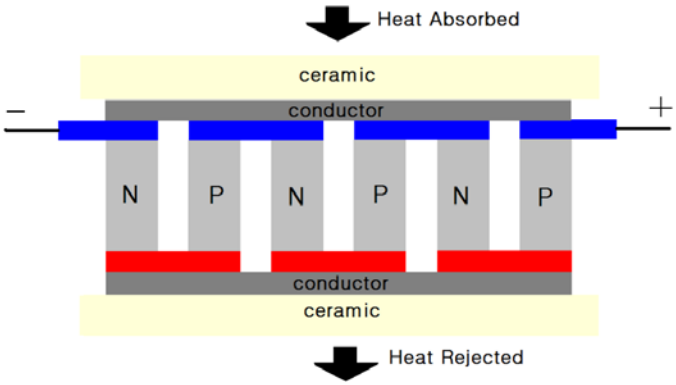

Figure 4: Diagram of thermoelectric Peltier cooling device

Heat Transfer Analysis

Transfer of heat from a load to the environment is a function of conduction and convection. Conduction is the transfer of heat through matter and is a function of the temperature difference across the material, physical dimensions, and thermal conductivity of the material. Convection is heat transfer across the boundary of air at the surface of the material and is a function of the temperature difference across the boundary layer and the rate of air movement at the surface.

When a moving fluid comes into contact with a surface at some temperature difference the fluid will transfer heat to or from the surface and advect heat away from the point of contact by its motion. Newton's Law of Cooling provides a simple expression for this rate of convective heat transfer.

$$Q = hA\,(T_s - T_f) \tag{1}$$

Where Q is the rate of heat convected in watts; T_s is the temperature of the solid in C°; T_f if the temperature of the fluid in C°; A is the area of the surface in contact with the fluid in square meters; and h is the convective heat transfer coefficient in watts/ square meter-C°.

Many factors affect convective heat transfer such as its geometry, type of flow, boundary conditions, type of fluid used and its properties. In this experiment, forced convection occurs when fluid flow, induced by the syringe pump, moves through the chip. The flow of fluid through the chip can be classified as laminar or turbulent. The heat transfer coefficient, h, used for calculating forced convective heat transfer is determined through a correlation of the dimensionless numbers: Nusselt number, Nu, Reynolds number, Re, and Prandtl number, Pr.

$$Nu = hD/k \qquad Re = DVp/\mu \qquad Pr = \mu C/k \tag{2}$$

Where D is tube diameter in meters; V is characteristic fluid velocity in m/s; k is thermal conductivity of fluid in kJ/hr-m-K; ρ is fluid density in kg/m^3; C is the constant pressure specific heat of the flowing fluid in J / kg-K; and μ is fluid viscosity in N-s /m^s.

Thermographic Acquisition

As shown in Figure 5, Infrared thermography can determine the temperature at the walls of the fluidic circuit and in the fluidic flow without disturbing the system. The IR camera was connected to a computer via a USB cable and recorded video of the fluid flow through the chip using the thermographic data acquisition and analysis application, ExaminIR. The recorded video can then be enhanced by adjusting the temperature scale limits and changing how the color palette is mapped to the data. Temporal plots can be obtained from the recorded video by the placement of ROI (region of interest) cursors that record the average temperature value of a 3x3 box of pixels over a time period. This data can then be exported to Excel for further manipulation.

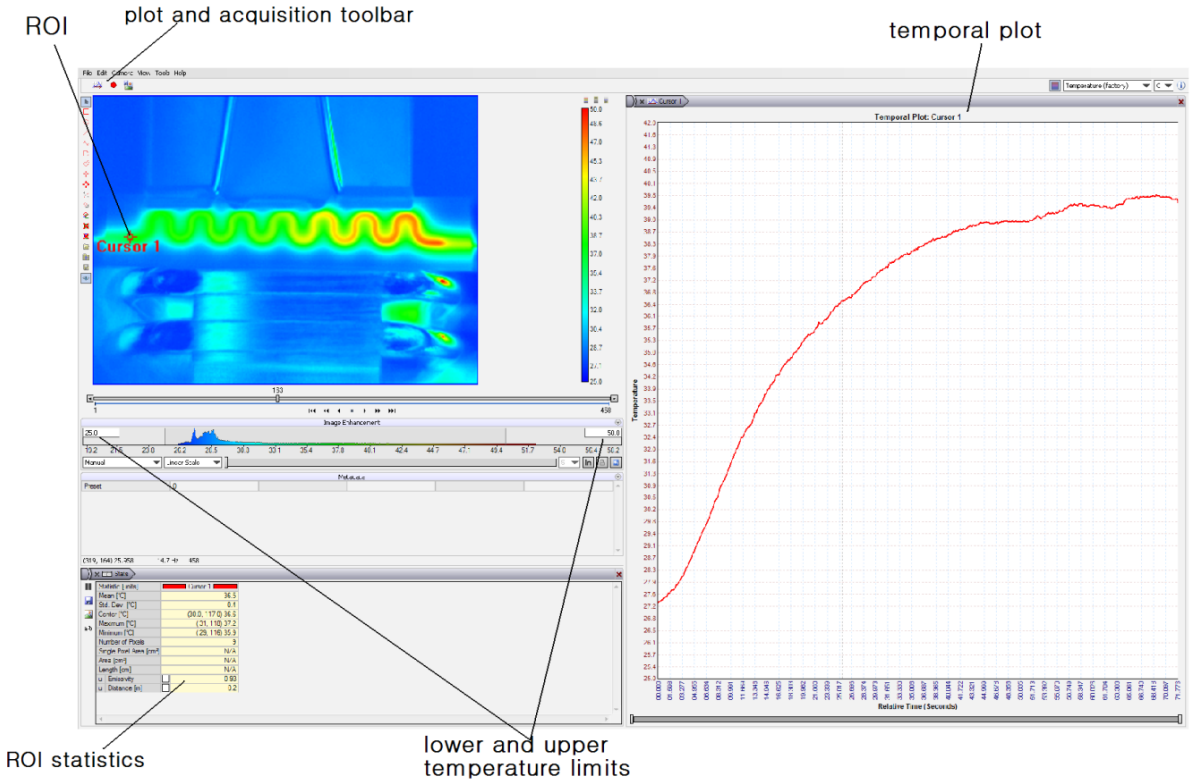

Figure 5: Screenshot of ExaminIR

The infrared camera is attached to a tripod and positioned directly above the microfluidic chip to record the fluid flow through the chip. The water flowed from right to left and inlet and outlet temperature values are recorded by placing ROI cursors in the middle of these ports as shown in Figure 6.

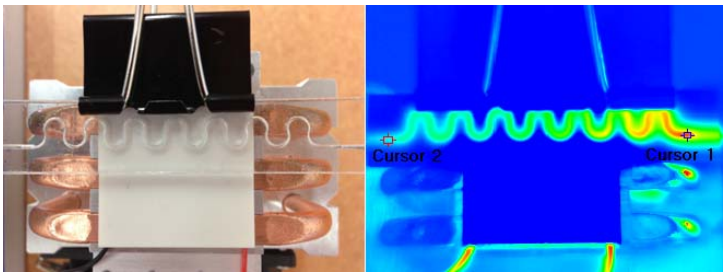

Figure 6: Normal IR image of fluid flow through the microfluidic chip on the Peltier cooling device

Thermal Image Analysis

At t=0 seconds, it was characteristic of the chip's inlet and outlet temperatures for all flow rates to begin at room temperature (25–27 °C) and increase until reaching thermal equilibrium. The temperature in the inlet and outlet ports of the chip was constantly changing as heat was absorbed by the thermoelectric cooling device and rejected to the heat sink. Thermal equilibrium was reached by the system when the inlet and outlet temperatures remained steady. The time it took the system to reach equilibrium decreased as the flow rate increased.

When the thermoelectric device was turned off, the heat transfer was a result of forced convection. When a moving fluid comes into contact with a surface at some temperature difference the fluid will transfer heat to or from the surface and advect heat away from the point of contact by its motion. Figure 7 shows the water flowing through the fluidic circuit gradually transferring heat to the chip, which is at room temperature, until equilibrium is reached.

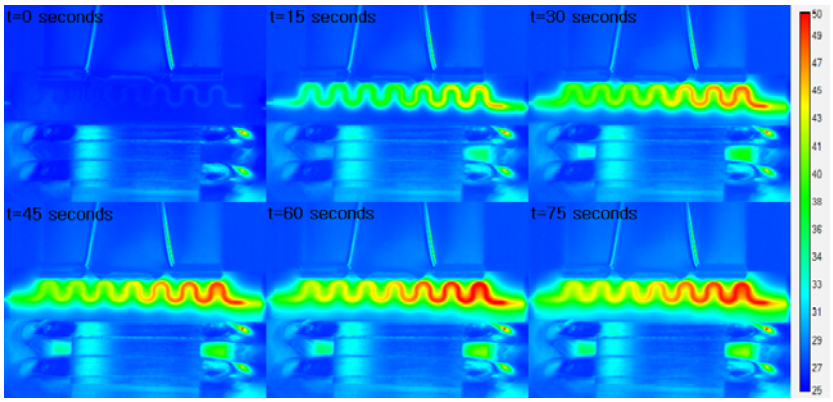

Figure 7: Sequence showing fluid flow without thermoelectric cooling.

There existed a greater temperature difference between the inlet and outlet ports when the thermoelectric cooling device was turned on because the thermoelectric cooling device was able to reject a greater amount of heat from the water flowing in the chip to the heat sink in order to decrease the outlet port temperature. Figure 8 shows how the thermoelectric device keeps the chip from heating up by absorbing the heat on the cold side of the thermoelectric and rejecting it to the hot side to be dissipated by the heat sink. It is also worth noting that when the thermoelectric device is on, the outlet temperature first decreases between the interval t=0 to t=10 seconds and then increases until thermal equilibrium. The outlet temperature decreases by less in this interval as the flow rate increases.

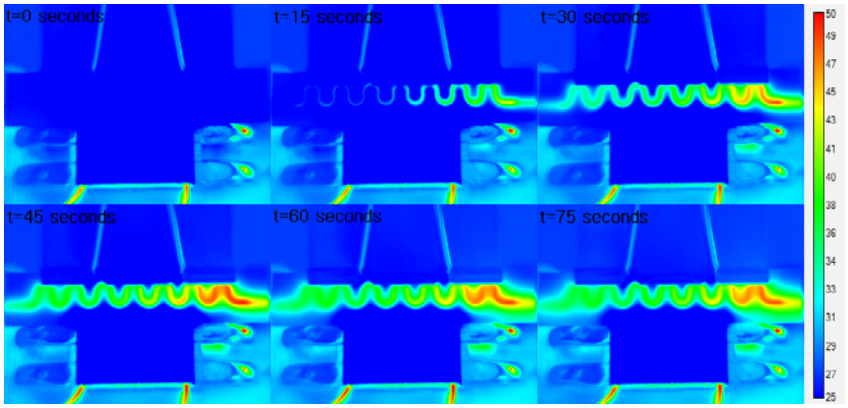

Figure 8: Sequence showing fluid flow with thermoelectric cooling.

When the chip reached thermal equilibrium, the inlet temperatures were the same for each flow rate regardless of whether the thermoelectric cooling device was on or off. Figures 9, 10, and 11 show that for the low flow rate the inlet temperature was 40°C when the thermoelectric device was off and 40°C when the thermoelectric was on. The inlet temperatures increased as the flow rate increased and were approximately 40°C for the low flow rate, 45°C for the medium flow rate, and 50°C for the high flow rate.

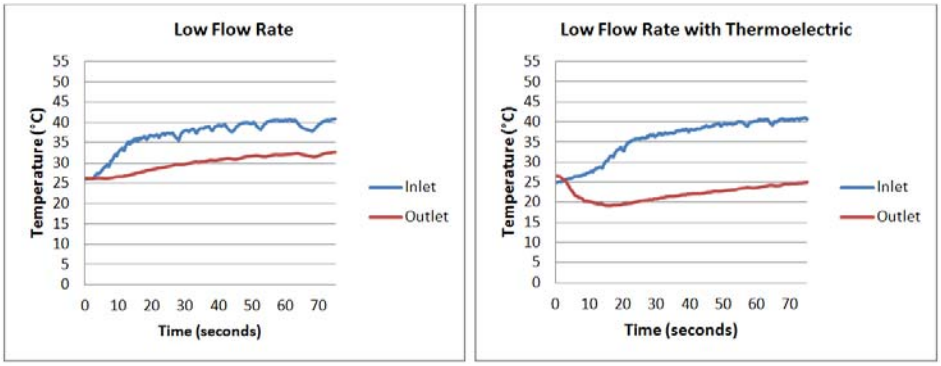

Figure 9: Temporal plots for low flow rate without and with a thermoelectric cooling device

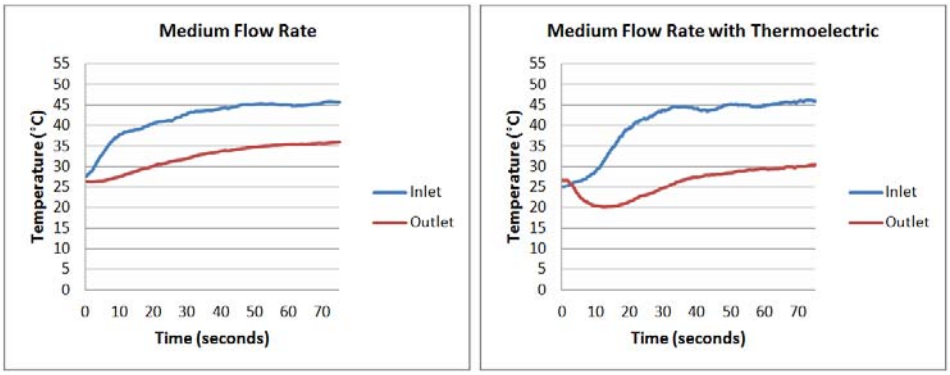

Figure 10: Temporal plots for medium flow rate without and with a thermoelectric cooling device

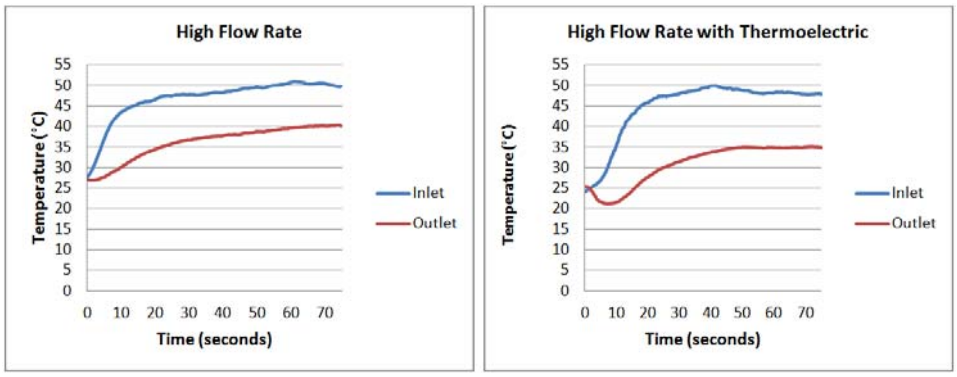

Figure 11: Temporal plots for high flow rate without and with a thermoelectric cooling device

Microfluidic System Operation and Data Acquisition. A programmable syringe pump delivered the cold and hot fluid to the fluidic circuit from two separate reservoirs. The 'cold' fluid reservoir was held at room temperature around 25-27° C. The 'hot' fluid reservoir was heated to approximately 40-41° C using a Peltier device supplied with a current of 1.25 amps. The experimental system allows for different flow configurations for performing different experiments. For example, the syringe pump enabled the experiment to be run at various flow rates and the interchangeable nature of the fluidic interconnections (micropipette tips) allowed for both co-current and counter current flow conditions. These versatilities in the way the experiment can be run made it possible to study the influences of each configuration on its temperature profile.

In order to image the chip, the infrared camera was positioned above the microfluidic chip using a tripod. The camera was connected to a computer via a USB cable where a thermographic data acquisition and analysis application called ExaminIR was used to capture and record video of fluid flow through the chip. The recorded video was then enhanced by adjusting the temperature scale limits and changing how the color palette was mapped to the data. Temperature measurements were obtained from the recorded video by the placement of ROI (region of interest) cursors that displayed the average temperature over time of a 3x3 box of pixels. The x and y values of the temporal plots were then exported to Excel for further manipulation. The experimental setup consists of a microfluidic chip that features two separate fluid channels (cold and hot). Tubes are connected to each inlet/outlet port of the chip via micropipette tips. A programmable syringe pump delivered the cold and hot flows to the fluidic circuit from two separate reservoirs held at constant temperatures. The 'cold' fluid reservoir was held at room temperature around 25° C. The 'hot' fluid reservoir was heated to approximately 65° C using a hot plate.

The experimental system allows for different flow configurations for performing different experiments. For example, the syringe pump enabled the experiment to be run at various flow rates and the interchangeable nature of the fluidic interconnections (micropipette tips) allowed for both parallel and counter flow conditions. These versatilities in the way the experiment can be run made it possible to study the influences of each configuration on its temperature profile as shown in Figure 12.

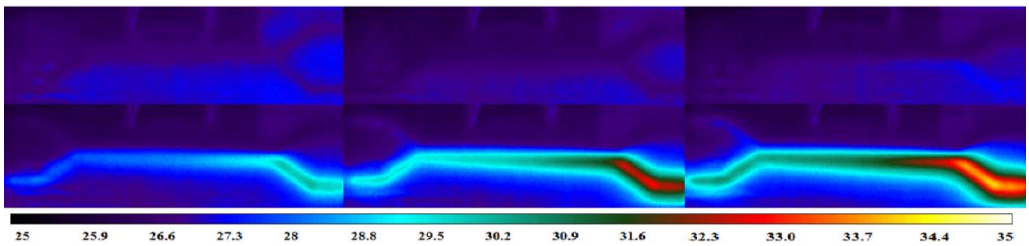

Figure 12: Sequence captured from ExaminIR showing a cold fluid (top) and hot fluid (bottom) flowing from right to left

The infrared camera was positioned above the microfluidic chip using a tripod and was connected to a computer via a USB cable. ExaminIR, a thermographic data acquisition and analysis application, was used to capture and record video of fluid flow through the chip. The recorded video was then enhanced by adjusting the temperature scale limits and changing how the color palette was mapped to the data. Temperature measurements were obtained from the recorded video by the placement of ROI (region of interest) cursors that displayed the average temperature over time of a 3x3 box of pixels. The x and y values of the temporal plots were then exported to Excel for further manipulation.

Results & Discussion on Energy Efficiency

There are several different ways to analyze the data from an infrared camera due to the fact that temperature measurements can be obtained across the entire image. There is flexibility in the analysis of infrared images because measurements are not limited to a single spot. Measurements can be obtained from the inlet and outlet channels or anywhere along the surface of the chip. Below are several examples of different analyses resulting from different placement and types of ROI cursors. The average temperature of the gradient was measured using a "box" ROI that measured the average temperature across the selected area for the 2 mL/min flow rate in the co-current configuration. The average temperature of the gradient increased approximately 3.25 °C in 4 minutes from 28.5 to 31.75 °C. The Average Temperature of Gradient vs. Time (for 2 mL/min flow rate in co-current configuration) is shown in Figure 13.

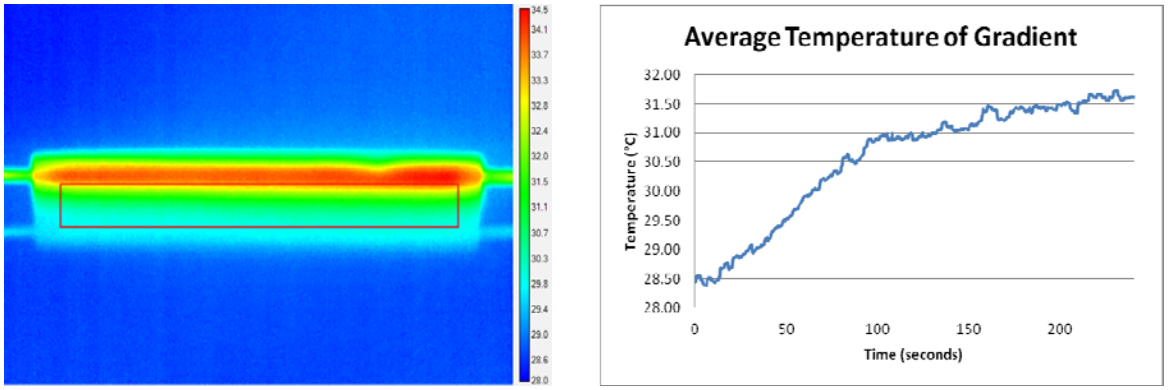

(a) (b)

Figure 13: (a) An ROI box indicating the area and (b) Average temperature measured

An ROI was placed at 3 mm increments between the hot and cold fluid channels in order to measure the chip's temperture vertically. Figure 14 shows the graph of vertical Distance between Fluid Channels vs. Temperature for 2 mL/min flow rate in co-current configuration. Four ROI cursors were used in total and were located 3, 6, 9 and 12 mm from the bottom of the chip. A somewhat linear relationship exists between vertical distance and temperature.

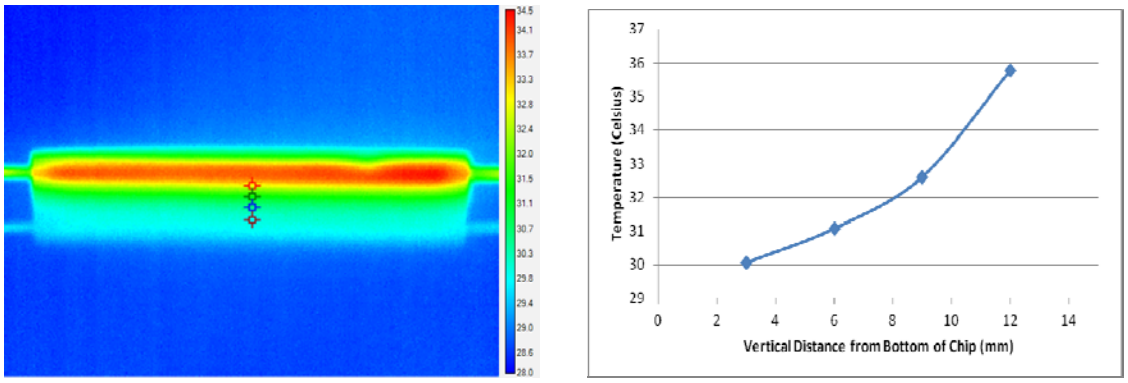

(a) (b)

Figure 14: (a) ROI cursors indicate the locations and (b) Temperature was measured for the 2 mL/min flow rate in the counter-current configuration

In Figure 15, a single ROI cursor was placed in the center of the chip in between the hot and the cold fluid channels to measure the temperature a sample would be heated to. This process was repeated for each flow rate (1, 2, and 4 mL/min) in each configuration (co-current and counter current). These plots show that the temperature increased as the flow rate increased.

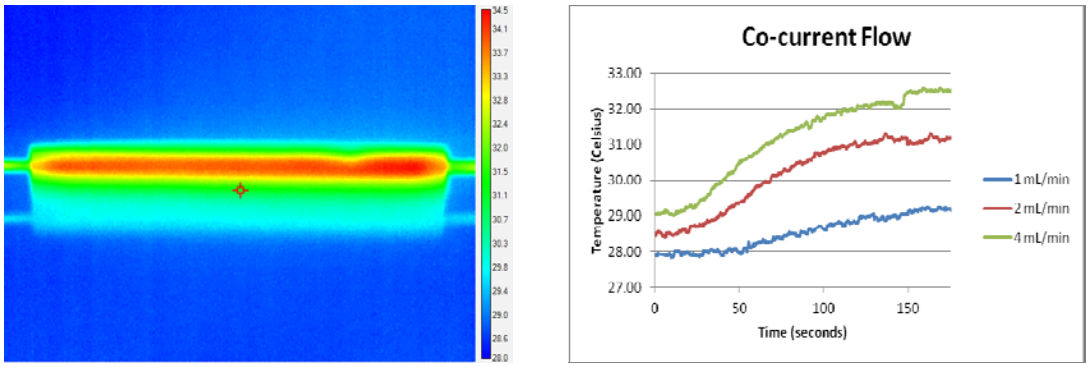

(a) (b)

Figure 15: (a) A single ROI cursor indicating the location where temperature was measured (b) for each flow rate (1, 2, and 4 mL/min) in each configuration (co-current and counter current)

Figure 16 shows the the graph of Temperature Profiles and Effectiveness Values versus distance for 2 mL/min flow rate in co-current configuration. The temperature profile in Figure 16 describes the inlet and outlet temperatures of the chip when it is operating in steady state. The temeprature profile shows that the temperatures decrease for both hot and cold fluid channels. The effectivness of the microfluidic chip was calculated using the equation:

$$\varepsilon = (t_{in} - t_{out}) / (T_{in} - T_{out}) \quad (3)$$

where ε is the calculated effectivenss value, T_{in} is the inlet temperature of the hot fluid, T_{out} is the outlet temperature of the hot fluid, t_{in} is the outlet temperature of the cold fluid, and t_{out} is the outlet tmeperature of the cold fluid. The effectiveness value represents the amount of heat transferred between the hot and cold fluid channels. Figure 17 shows the heat trasfer efficiency vs time based on Equation (3). It indicates that there was heat transfer between the two fluids. This was most likely due to the large distance between the fluid channels. Decreasing this distance would result in a larger effectiveness value.

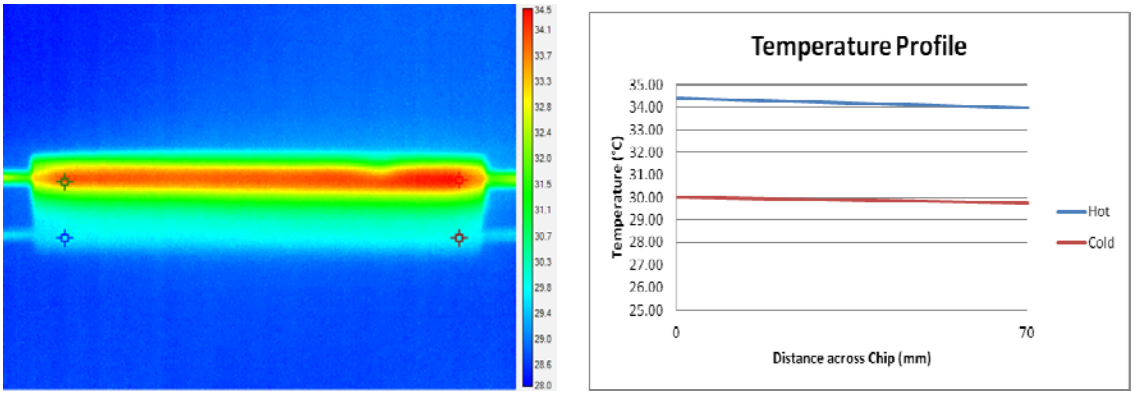

Figure 16: (a) ROI cursors indicating the locations where (b) temperature profile measured in the inlet and outlet for both the hot and cold fluid channels

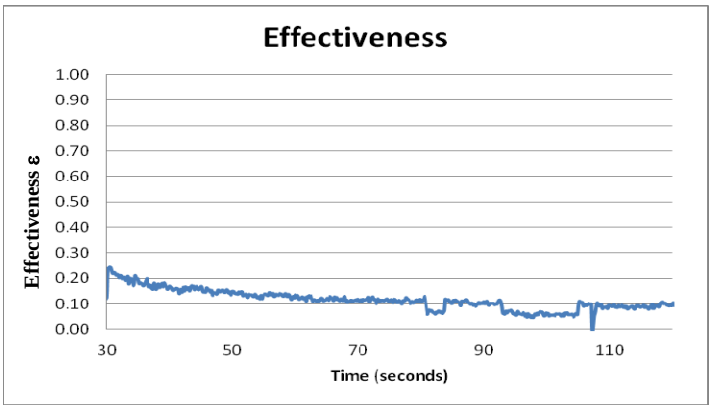

Figure 17: Calculated energy efficiency of microfluidic chip operating in the co-current configuration

Real-time Infrared Thermography Measurement Experiment for Students

The infrared thermography measurement experiment has been developed for the courses MET 100 Graphics Communication, MET 101 Manufacturing Materials and MET 205 Robotics and Mechatornics as a part of this laboratory development. The course provides the students with a

comprehensive knowledge of micro-manufacturing energy efficiency using infrared thermography measurement laboratory as shown in Figure 18. The specific real-time infrared thermography methodologies chosen are related to computers and networks, energy monitoring, and infrared camera. The laboratory assignment was used to reinforce lecture information and to give hands-on experience on solar cell quality. It is believed that the student learning experience about an infrared imaging analysis for micro-manufacturing is enhanced.

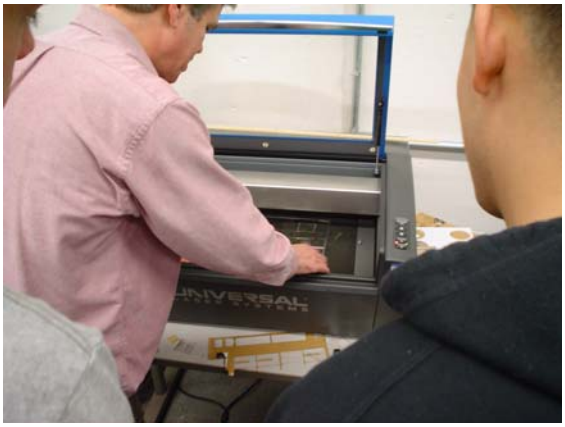

Figure 18: Students performing Infrared thermography measurement as for monitoring energy efficiency issues in micro-manufacturing

Assessment and Evaluation

The main student learning outcomes are focused on (1) learning through real-time energy efficiency measurement; (2) manufacturing process inspection and evaluation; (3) real data analysis; (4) development of lab-on-a-chip projects based on experimental data; (5) validation of the green energy manufacturing laboratory models through several student projects. We also continuously improved the experimental activities as well as the teaching modules based also on student project evaluations. The questionnaire is designed to reflect the students' understanding of the overall micro manufacturing energy system and target the benefits of technologies for high precision engineering applications. The histograms in Figure 19 demonstrate the evaluation results for the questionnaire provided to the students. The students evaluate the following question statements on the scale from1 to 5, where 1 indicates "strongly disagree" and 5 indicates "strongly agree."

1. I have grasped the green manufacturing energy concepts through the "energy efficiency measurement" experiment.
2. I have collected appropriate evidence (data) from my experiments in the lab.
3. I could accurately interpret the results from the statistical evaluation I had performed.
4. I was able to make effective decisions and improve the processes based on my analysis.
5. The course has provided me with the familiarity of energy measurement methods including thermal imaging equipment and data analysis techniques in situations representative of typical energy problems encountered on the shop or factory floor.

6. The instructor has provided accurate and easy to understand instructions for the lab experiments.
7. The instructor has provided enough time for the lab experiments.
8. The lab equipment was easy to operate.
9. In my opinion, the energy measurement methods have many applications in practice.

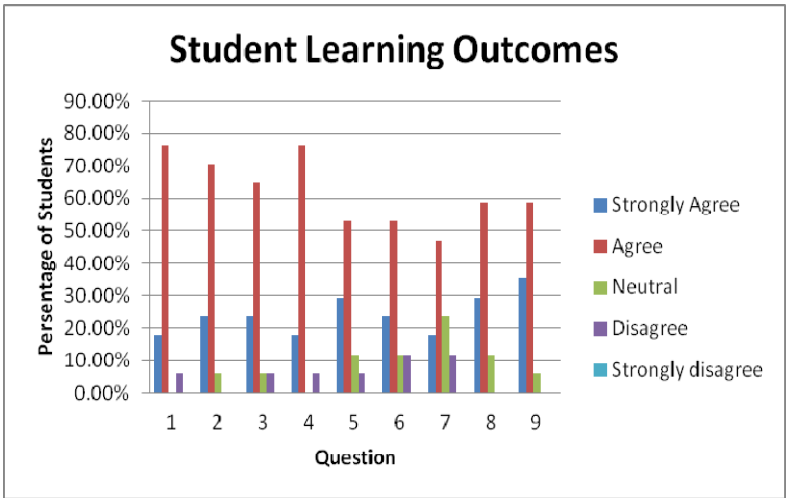

Figure 19: Student learning evaluations

Since the implementation of these experimental activities as basis for teaching energy measurement methods, the student evaluations have been consistently high with an average of 4.31 out of 5.00. Overall the feedback received at the end of the term from the participating students was largely positive with regards to the experiments involving green energy manufacturing systems. Students were exposed tremendously to new theories, applications and technologies that are still considered emerging technologies and are not in a textbook or course notes. In this way we stimulated students further to seek research activities based on their personal or career interests through open-ended problem solving, interdisciplinary projects, offering them a great opportunity to "try-out" at a smaller scale a "capstone type" projects. Students enriched constantly their knowledge and they proved critical thinking and creativity. Some of the main drawbacks pointed out by the students include the fact that since the devices are extremely small it is difficult at times for all students to directly work hands-on with the experiment and hence it may be better suited for an individual or much smaller lab group than the 3-5 students pairing used this past term. Furthermore, majority of students (~80%) developed a special interest in the biomedical and micro manufacturing applications for this technology. Other applications such as electronic cooling could be further discussed and emphasized to broaden the impact of this experiment.

Conclusion

Imaging (both visible and infrared) of microfluidic devices can be used to study fluid flow and thermal phenomena in educational laboratories for undergraduate engineering courses. The experiments described here are representative of projects that combine microsystems, image processing, rapid prototyping, and instrumentation with various sensors in an integrated system. Microfluidic devices, made in clear plastic and measuring several centimeters on a side with flow channel features on the order of 0.1 mm to several mm, loaded with dyed liquids, are well-suited for image capture and

subsequent image processing and analysis in order to characterize the flow. Similarly, temperature profiles of microfluidic devices show various thermal and phase change effects. Microfluidics-based experiments allow students to work from design through prototype to test in time frames appropriate for educational purposes, and with modest demands on resources.

Acknowledgements

This work has been supported by the NSF TUES Type 1 project 1044708 and the US Department of Education under the joint DHSIP Program with the University of Texas at El Paso, PR/Award No.: P031S120131. The authors wish to express sincere gratitude for their financial support.

Bibliography

1. H. BECKER AND C. GÄRTNER [2008], "Polymer microfabrication technologies for microfluidic systems" *Anal. Bioanal. Chem.* **390** 89-111.
2. I.BLACK [1998], "Laser cutting of Perspex" *J. Materials Science Letters* **17** 1531-1533.
3. F. Caiazzo, F. Curcio, G. Daurelio, F. Memola Capece Minutolo [2009], "Laser cutting of different polymeric plastics (PE, PP and PC) by a CO2 laser beam" *J. Materials Processing Technology* **159** 279-285.
4. T.A. FRANKE and A. WIXFORTH [2008], "Microfluidics for miniaturized laboratories on a chip" *ChemPhysChem* **9**, 2140-2156.
C. HABER [2006], "Microfluidics in commercial applications: An industry perspective" *Lab on a Chip* **6, 9** 1118-1121.
5. Y.-C. HSU and T.-Y. CHEN [2007] "Applying Taguchi methods for solvent-assisted PMMA bonding technique for static and dynamic μ-TAS devices" *Biomedical Microdevices* 9513-9522.
6. T-.W. Lee [2008], *Thermal and Flow Measurements* (CRC Press, Boca Raton, Florida).
7. A. McAndrew [2004], *Introduction to Digital Image Processing with MATLAB*® (Thompson).
8. K.-I. OHNO, K. TACHIKAWA, and A. Manz [2008], "Microfluidics: Applications for analytical purposes in chemistry and biochemistry" *Electrophoresis* **29** 4443-4453.
9. N. PAMME [2006], "Magnetism and microfluidics" *Lab on a Chip* **6** 24-28.
10. L. ROMOLI, G. TANTUSSI, and G. DINI [2011], "Experimental approach to the laser machining of PMMA substrates for the fabrication of microfluidic devices" *Optics and Lasers in Engineering* **49** 419-427.
11. D. SNAKENBORG, H. KLANK, and J.P. CUTLER [2004], "Microstructure fabrication with CO_2 laser system" *J. Micromech. Microeng.* **14** 182-189.
12. C.-W. TSAO and D.L. DEVOE [2009], "Bonding of thermoplastic polymer microfluidics" *Microfluidics Nanofluid.* **6** 1-16.
13. F. UMBRECHT, D. MÜLLER, F. GATTIKER, C.M. BOUTRY, J. NEUENSCHWANDER, U. SENNHAUSER, and CH. HIEROLD [2009], "Solvent assisted bonding of polymethylmethacrylate: Characterization using the response surface methodology" *Sensors and Actuators A*: *Physical* **156** 121-128